



Published in final edited form as:

J Pain. 2012 September ; 13(9): 836–848. doi:10.1016/j.jpain.2012.05.013.

Spinal cannabinoid receptor type 2 agonist reduces mechanical allodynia and induces mitogen-activated protein kinase phosphatases in a rat model of neuropathic pain

Russell P. Landry^{a,d}, Elena Martinez^{a,d}, Joyce A. DeLeo^{a,b,c}, and E. Alfonso Romero-Sandoval^{a,b,*}

^aDartmouth Medical School, Department of Anesthesiology, Lebanon, New Hampshire, USA

^bDepartment of Pharmacology/Toxicology, Dartmouth Medical School, Hanover, New Hampshire, USA

Abstract

Peripheral nerve injury generally results in spinal neuronal and glial plastic changes associated with chronic behavioral hypersensitivity. Spinal mitogen-activated protein kinases (MAPKs), e.g., p38 or extracellular signal-regulated kinases (ERKs), are instrumental in the development of chronic allodynia in rodents, and new p38 inhibitors have shown potential in acute and neuropathic pain patients. We have previously shown that the cannabinoid type 2 receptor agonist JWH015 inhibits ERK activity by inducing MAPK phosphatase (MKP)-1 and MKP-3 (the major regulators of MAPKs) in vitro in microglial cells. Therefore, we decided to investigate the role of these phosphatases in the mechanisms of action of JWH015 in vivo using the rat L5 nerve transection model of neuropathic pain. We observed that peripheral nerve injury reduced spinal MKP-1/3 expression and activity and that intrathecal JWH015 reduced established L5 nerve-injury-induced allodynia, enhanced spinal MKP-1/3 expression and activity, and reduced the phosphorylated form of p38 and ERK-1/2. Triptolide, a pharmacological blocker of MKP-1 and MKP-3 expression, inhibited JWH015's effects, suggesting that JWH015 exerts its antinociceptive effects by modulating MKP-1 and MKP-3. JWH015-induced antinociception and MKP-1 and MKP-3 expression were inhibited by the cannabinoid type 2 receptor antagonist AM630. Our data suggest that MKP-1 and MKP-3 are potential targets for novel analgesic drugs.

Keywords

CB2 receptors; MKP; pain; spinal cord; MAPK

© 2012 The American Pain Society. Published by Elsevier Inc. All rights reserved.

*Corresponding author: Edgar Alfonso Romero-Sandoval, M.D., Ph.D., edgar.a.romero-sandoval@dartmouth.edu, Address: One Medical Center Drive, DHMC – HB7125, Lebanon, New Hampshire 03756, USA, Phone: 603-650-6003, Fax: 603-650-8525.

^c(current affiliation) Department of Biology, Emmanuel College, Boston, Massachusetts, USA.

^dThese authors contributed equally to this study.

DISCLOSURES

The authors would like to acknowledge the American Pain Society 2008 Future Leaders in Pain Research Small Grants, the Rita Allen Foundation & American Pain Society 2011 Pain grant (AR-S), Hitchcock Foundation award 2011–2012, and the National Institute of Drug Abuse DA025211 (AR-S) and DA11276 (JAD) for funding. The authors declare no conflict of interest.

Publisher's Disclaimer: This is a PDF file of an unedited manuscript that has been accepted for publication. As a service to our customers we are providing this early version of the manuscript. The manuscript will undergo copyediting, typesetting, and review of the resulting proof before it is published in its final citable form. Please note that during the production process errors may be discovered which could affect the content, and all legal disclaimers that apply to the journal pertain.

INTRODUCTION

Chronic neuropathic pain is very difficult to treat. A better understanding of the mechanisms that drive chronic pain is necessary to develop new strategies for treating or preventing chronic pain.

In rodent models of pain, peripheral nerve injury produces molecular changes in the spinal cord that are associated with chronic allodynia. One of the better-characterized molecular pathways affected in spinal cord in rodent models of pain is the mitogen-activated protein kinase (MAPK) signaling pathway. Induction and long-lasting spinal cord phosphorylation of MAPKs following peripheral nerve injury are instrumental in developing and maintaining chronic hypersensitivity.¹⁵

The clinical relevance of MAPKs in pain conditions has been supported by recent clinical trials showing that novel p38 inhibitors, which have relatively safe side-effect profiles, reduce postoperative pain³⁵ and neuropathic pain⁴ in patients. However, the role of extracellular signal-regulated kinases (ERKs) in patients with pain remains to be studied. Inhibition of MAPKs results in a reduction of downstream factors (cytokines, chemokines, nitric oxide, etc.) in immunocompetent cells^{20, 21} and reduces the excitability of neurons in the spinal cord.²⁰ Therefore, strategies directed to control MAPK phosphorylation have the potential to improve pain conditions.

We have previously shown that the cannabinoid type 2 (CB2) receptor agonist JWH015 produces antinociception in a dose-dependent manner in a rat model of neuropathic pain.³⁰ Additionally, we have observed that JWH015 reduces the phosphorylated form of ERK (p-ERK) by inducing MAPK phosphatase (MKP)-1 and MKP-3 in vitro in primary microglial cells.³¹ We hypothesize that positive modulation of MKPs is part of the mechanism by which JWH015 reduces allodynia induced by peripheral nerve injury in rats.

There are 16 identified dual-specificity MKPs, among them MKP-1 and MKP-3, the major regulators of MAPKs.¹⁴ MKP-1 is an immediate early gene, while MKP-3 requires a longer time to be induced.¹⁴ Dephosphorylation of MAPKs by dual-specificity phosphatases (i.e., MKPs) reduces pro-inflammatory factor production, promoting the resolution of inflammatory processes.¹⁴ Thus, some anti-inflammatory drugs—e.g., glucocorticoids—achieve their antinociceptive effects by inducing MKP expression.^{1, 33, 39} The relevance of MKPs in human conditions has been proven in studies demonstrating that MKP-1 polymorphisms alter the response to inhaled corticosteroids in asthmatic patients¹⁷ and that blood levels of MKP-1 are associated with post-operative morbidities.¹¹ However, the role of MKPs in pain conditions remains to be elucidated.

Different MKPs possess differential substrate preferences. Thus, MKP-1 dephosphorylates p-38 (preferentially), p-JNK and p-ERK,^{8, 39} while MKP-3 preferentially dephosphorylates p-ERK^{19, 22} and is able to dephosphorylate p-38 and p-JNK.¹⁴ We and others have demonstrated that MKP induction is the mechanism by which exogenous³¹ or endogenous⁸ cannabinoids induce anti-inflammatory phenotypes in glia. However, the role of phosphatases in the pathophysiological mechanisms that underlie the development and maintenance of chronic pain is unknown.

It has been shown that due to the enzymatic nature of MKPs, their levels of expression and activity determine the prevalence of the activated (phosphorylated) forms of MAPKs.^{10, 14} Therefore, it is possible that a disruption in MKP activity or expression determines, at least partially, the persistent phosphorylation of spinal MAPKs in rodent models of neuropathic pain¹⁶ or in rodent models of acute postoperative pain that transitions to persistent

postoperative pain.³⁷ Accordingly, the current study also aims to determine the expression and activity of MKP-1 and MKP-3 in spinal cord following peripheral nerve injury.

Our studies clarify the role of MKPs in the pathophysiological mechanisms of neuropathic pain in this rat model and highlight the potential of these molecules as targets for the development of drugs with novel mechanisms of action to treat or prevent chronic pain.

MATERIALS AND METHODS

Animals, surgeries, behavior testing, and drugs

The Institutional Animal Care and Use Committee at Dartmouth College approved all animal procedures. Additionally, all procedures were in accordance with the Guidelines for Animal Experimentation of the International Association for the study of Pain. Male Sprague-Dawley rats weighing 250–300 g (Harlan, Indianapolis, IN) were housed individually and maintained in 12:12 h light-dark cycle with *ad libitum* access to food and water. Animals were randomly divided into one of two procedures, L5 nerve transection (L5NT) or sham surgery as previously described.³⁰ Briefly, rats were anesthetized with 2% isoflurane in O₂ and a small incision was made between the L5 and S1 region. The L6 transverse process was removed, and the L5 spinal nerve was identified. In the L5NT group, the L5 nerve was transected, and in the sham group the L5 nerve was left undisturbed. The incision was then closed, and the animals were returned to their housing. Mechanical allodynia was assessed in the ipsilateral paw to surgery using Von Frey filaments (Stoelting, Wood Dale, IL) and the up-down statistical method.⁷ The 50% paw-withdrawal threshold was then calculated. Behavioral tests were performed in all animals before surgery (baseline) and four days after surgery (before treatment). The CB2 receptor agonist JWH015, MKP-1 and MKP-3 antagonist triptolide, and CB2 receptor antagonist AM630 were obtained from Tocris, Ellisville, MI. Drugs were diluted in dimethylsulfoxide (DMSO) and then in saline (1:1). Animals were randomly divided into one of the treatment groups. Drugs and/or vehicle were administered intrathecally (i.t.) and concomitantly in a final volume of 20 μ L four days after surgery, and their behavioral effects (withdrawal thresholds) were evaluated 30 and 60 min after their injection. The investigator was blinded to drug treatment in all experiments. Behavioral experiments were performed in three different sessions and having at least one animal per condition or treatment in every session. The following groups were included in the study: L5 nerve transection (L5NT) +JWH015+vehicle ($n = 6$), L5NT+JWH015+triptolide ($n = 6$), L5NT+JWH015+AM630 ($n = 4$), L5NT+vehicle+vehicle ($n = 3$), and sham+vehicle+vehicle ($n = 3$). We have previously demonstrated that JWH015 produces a dose-dependent antinociceptive effect in the L5 nerve transection model that we used in this study.³⁰ Based on these data, we decided to use a 50- μ g dose of JWH015. This is an antinociceptive CB2 receptor-selective dose that does not produce cannabinoid psychotropic side effects.³⁰ For AM630, we used a dose that we have previously observed to block CB2 receptor effects, i.e., 50 μ g.² For triptolide, based on a pilot study we chose a similar dose to the one used for JWH015, i.e., 50 μ g. Triptolide has been shown to reduce inflammatory products *in vitro*;⁹ in low doses (2.5 μ g, i.t.) it may induce antinociception *in vivo*.²³ However, we have demonstrated that triptolide alone does not modify MKP-1, MKP-3, or MAPKs in lipopolysaccharide-stimulated microglial cells.³¹ Moreover, our laboratory and others have shown that triptolide effectively blocks MKP-1 and MKP-3 when the expression of these MKPs is enhanced, and consequently blocks pharmacological anti-inflammatory effects *in vitro*.^{12, 38} Due to the lack of more specific pharmacological tools, triptolide is an accepted and widely used MKP blocker for multiple settings.^{27, 29, 34, 39} To validate the use of triptolide as a MKP blocker, we performed Western blot analyses to test its effects in MKP protein expression and a phosphatase enzymatic activity assay as a confirmatory functional study, and measured levels of MKP

substrates (MAPKs) by Western blot analyses as additional confirmatory functional outcomes.

Western blot analysis

Rats were euthanized using isoflurane anesthesia (4% in oxygen) and decapitated, and the L5 region of the spinal cord was collected for further study. The spinal cord was sonicated in PBS containing 1:1,000 protease inhibitor (Sigma, St. Louis, MO). The sample protein concentrations were determined by DC assay (Bio-Rad, Hercules, CA) following manufacturer's instructions. Protein (50 µg) for each sample was brought to 35 µL total volume in 1X Lammeli Sample Buffer (Bio-Rad, Hercules, CA) with 2-mercaptoethanol and boiled at 100 °C for 5 min. The 35 µL of protein samples and 16 µL of standard protein markers (Bio-Rad, Hercules, CA) were subjected to SDS polyacrylamide gel electrophoresis and transferred to polyvinylidene difluoride membranes. The membranes were blocked for 1 h in 5% BSA with TBS-Tween 20 (0.05%, Sigma, St. Louis, MO), then incubated for 48 h at 4 °C in 5% BSA with TBS-Tween 20 and (a) monoclonal mouse anti-MKP-1 (1:500, Santa Cruz Biotechnology, Santa Cruz, CA), (b) rabbit anti-MKP-3 (1:500, Cell Signaling, Danvers, MA), (c) mouse anti-phospho-p38 (p-p38, 1:500, Cell Signaling, Danvers, MA), or (d) mouse anti-p-ERK-1/2 (p-ERK-1/2, 1:500, Cell Signaling, Danvers, MA). The blots were then washed three times in TBS-Tween 20 for 10 min and then incubated for 1 h in goat anti-mouse or goat anti-rabbit HRP-conjugated antibody (1:3000, Pierce, Rockford, IL). Thereafter, the blots were washed three times in TBS-Tween 20 for 10 min, treated with SuperSignal West Femto Maximum Sensitivity Substrate (Thermo Fisher Scientific, Rockford, IL) for 5 min, and then imaged with a Syngene G-Box (Synoptics, Frederick, MD). The membranes were stripped for 25 min and re-probed with mouse anti-Beta actin (1:3,000, Abcam, Cambridge, MA), rabbit anti-total-p38 (t-p38, 1:1000, Cell Signaling, Danvers, MA), or rabbit anti-total-ERK (t-ERK-1/2, 1:500, Cell Signaling, Danvers, MA) overnight at 4 °C. Band density was quantified using Syngene Tools software (Synoptics, Frederick, MD).

Immunohistochemistry

Animals were anesthetized in 2–3% isoflurane in O₂ then transcardially perfused using 10 mM PBS (200 mL) followed by 4% formaldehyde (400 mL). The L5 region of the spinal cord was removed and put in 30% sucrose for 48 h at 4 °C. The tissues were then mounted in optimal cutting temperature compound (Sakura Finetek, Torrance, CA), and frozen at –80 °C until further use. The L5 spinal cord sections were transversely cut to 20 µm thickness, then blocked for 1 h in 5% normal goat serum (NGS, Vector Labs, Burlingame, CA) and 0.01% Triton X-100 (Sigma, St. Louis, MO) in PBS.

For the single staining of MKP-1 or MKP-3, the following procedures were performed: The sections were incubated overnight in monoclonal mouse anti-MKP-1 (1:100, Santa Cruz Biotechnology, Santa Cruz, CA) or rabbit anti-MKP-3 (1:100, Cell Signaling, Danvers, MA) in PBS with 1% NGS and 1% Triton X-100. The tissues were then washed three times for 10 min in PBS. The MKP-1 tissues were incubated for 1 h in goat anti-mouse biotin-conjugated antibody (1:3,000, Thermo Scientific, Pittsburgh, PA), then washed three times for 10 min in PBS, then processed using the Vector ELITE ABC kit (Vector Labs, Burlingame, CA). A DAB tablet was dissolved in PBS, then filtered, and 15 µL of H₂O₂ was added to the DAB solution. The tissues were placed in the DAB solution for 2 min. The sections were then mounted on a slide and left to dehydrate for 10–20 min at room temperature. The mounted tissue was placed two times in 95% ethanol, two times in 100% ethanol, and once in 100% Xylene all for 5 min each. Finally the tissues were sealed in Permount (Fischer, Franklin, MA). The MKP-3 tissues were incubated for 1 h in goat anti-rabbit Alexa 488 (1:250, Invitogen, Grand Island, NY). The sections were then washed three

times in PBS for 10 min, then mounted on slides in VectorShield mounting medium (Vector Labs, Burlingame, CA).

For the dual staining, the following procedures were performed: For the MKP-1, the tissues were incubated overnight in monoclonal mouse anti-MKP-1 (1:100, Santa Cruz Biotechnology, Santa Cruz, CA) with either rabbit anti-NeuN/Fox3 (NeuN, 1:10,000, neuron nuclear marker, Biosensis, Australia), or rabbit anti-GFAP (glial fibrillary acidic protein, marker for astrocytes, 1:400, Sigma, St. Louis, MO) in PBS with 1% NGS and 1% Triton X-100. The sections were washed three times for 10 min and incubated for 1 h in goat anti-rabbit Alexa 555 and goat anti-mouse Alexa 488 (1:250, Invitrogen) diluted in PBS with 1% NGS and 1% Triton X-100. The tissues were then washed three times for 10 min and mounted on slides in VectaShield mounting medium (Vector Labs, Burlingame, CA).

To avoid cross-reactivity when co-staining with primary antibodies against MKP-1 and ED2 that are both mouse-derived, a TSA Signal Amplification Kit was used following the manufacturer instructions (PerkinElmer LifeSciences Inc, Boston, MA). First, the tissues were incubated overnight in monoclonal mouse anti-MKP-1 (1:5000, Santa Cruz Biotechnology, Santa Cruz, CA) in 1% NGS and 1% Triton X-100. This concentration of anti-MKP-1 did not produce any visible staining when incubated with secondary antibody anti-mouse Alexa 488 without any amplification procedure (see description for control staining below). The next day, a TSA Signal Amplification Kit (PerkinElmer LifeSciences Inc, Boston, MA) was used, following the manufacturer's instructions. The tissues were washed twice for 5 min in PBS, then incubated in a biotinylated goat anti-mouse secondary antibody (1:3,000, Vector Labs, Burlingame, CA) for 1 h at 4 °C. The sections were then washed, incubated in SA-HRP (1:100) for 1 h at 4 °C, washed again, and incubated in the TSA fluorophore (1:250) for 10 min at 4 °C. The tissues were then washed again and incubated overnight in mouse anti-ED2 (marker for microglia, 1:150, Serotec, Raleigh, NC) in PBS with 1% NGS and 1% Triton X-100. The sections were washed three times for 10 min, and then incubated for 1 h in goat anti-mouse Alexa 555 secondary antibodies (1:250, Invitrogen, Grand Island, NY) in PBS with 1% NGS and 1% Triton X-100. The tissues were then washed three times for 10 min and mounted on slides in VectaShield mounting medium (Vector Labs, Burlingame, CA). The following control staining groups were included to test MKP-1 antibody signal amplification using the TSA kit: (a) 1:5000 MKP-1 primary antibody alone and the 1:250 goat anti-mouse secondary antibody Alexa 555, which confirmed no red fluorescent staining, (b) 1:5000 anti-MKP-1 primary antibody and the TSA kit, which showed distinct green MKP-1 fluorescent staining, and (c) the TSA kit, the mouse anti-ED2 primary antibody, and the goat anti-mouse Alexa 555 secondary antibody, excluding the MKP-1 primary antibody, which provided green fluorescent background of the TSA kit and distinct red fluorescence of the ED2 antibody. The controls confirmed the specificity of the complete co-stain, as we have previously described in detail.³

For the MKP-3, the sections were incubated overnight in rabbit anti-MKP-3 (1:100, Cell Signaling, Danvers, MA) with either rabbit anti-NeuN/Fox3 (NeuN, 1:10,000, neuron nuclear marker, Biosensis, Australia), mouse anti-GFAP (1:10,000, Dako, Carpinteria, CA), or mouse anti-ED2 (1:150, Serotec, Raleigh, NC) in PBS with 1% NGS and 1% Triton X-100. The sections were then washed three times for 10 min and incubated for 1 h in goat anti-rabbit Alexa 488 and goat anti-mouse Alexa 555 (1:250, Invitrogen, Grand Island, NY) in PBS with 1% NGS and 1% Triton X-100. The tissues were then washed three times for 10 min and mounted on slides in VectaShield mounting medium (Vector Labs, Burlingame, CA).

The specificity of each antibody was tested by omitting the primary antibody on one to three additional sections. The antibodies for MAPKs and cell markers are widely used due to their

proven specificity. To confirm the specificity of our MKP-1 antibody we used MKP-1-overexpressing BV-2 cells generated in our laboratory and observed that MKP-1 was robustly expressed in these cells when compared to normal or non-transfected BV-2 cells (Supplementary Figure 1). To confirm the specificity of our MKP-3 antibody we used MKP-3 knockout mice spinal cord tissue, and observed that MKP-3 was not expressed in this tissue when compared to wild type mice (Supplementary Figure 2).

The stained sections were examined with an Olympus fluorescence microscope and images were captured with a Q-Fire cooled camera (Olympus, Melville, NY). MKP-1 and MKP-3 expression in specific areas of dorsal horn spinal cord (laminae I–II and laminae III–V) was quantified using SigmaScan Pro 5 (SPSS, Chicago, IL) as the number of pixels above a preset intensity threshold within a normalized total pixel area, as we have previously described in detail.^{3, 30} Confocal microscopy of dual antibody immunofluorescence was performed with a Zeiss LSM 510 Meta confocal microscope (Englert Cell Analysis Laboratory of Dartmouth Medical School) and images were prepared with the Zeiss LSM software (Thornwood, NY) and Adobe Photoshop software (San Jose, CA).³ All images were taken from dorsal horn spinal cord ipsilateral to nerve injury.

MKP immunoprecipitation and phosphatase activity assay (p-nitrophenyl phosphate [pNPP] assay)

For these experiments spinal cord hemisections (dorsal and ventral horns) from the L5-L6 spinal cord region were used. Spinal cord protein (100 µg) was incubated overnight with 2 µg of mouse anti-MKP-1 (Santa Cruz Biotechnology, Santa Cruz, CA) or rabbit anti-MKP-3 (Cell Signaling, Danvers, MA) primary antibody at 4 °C. Then 20 µL of protein A/G resin (Santa Cruz Biotechnology, Santa Cruz, CA) was added and the samples were left on a shaker to incubate overnight at 4 °C. The samples were centrifuged and washed, then 20 µL was collected from the bottom of the tubes. Next, 50 µl of pNPP (50 mM) solution was added and incubated for 15 min at room temperature. The immunoprecipitated MKP-1 or MKP-3 activity was measured by ability to catalyze the hydrolysis of pNPP to p-nitrophenol, a chromogenic product with absorbance at 405 nm. NaOH (1 N, 50 µL) was added to quench the enzymatic activity. The amount of product, p-nitrophenol, was determined by reading the absorbance at 405 nm. Nonspecific hydrolysis of pNPP was assessed in the absence of tissue sample and this value was subtracted from the values using samples. The percentage of activity was calculated using the values for the control group (sham+vehicle) as 100%. In other experiments, the amount of MKP-1 or MKP-3 was quantified after immunoprecipitation using the DC assay (Bio-Rad, Hercules, CA) following manufacturer's instructions and the enzymatic activity was calculated per µg of protein. Additionally, pNPP assay was performed to determine the global unspecific phosphatase activity in 100 µg of spinal cord tissue from all the groups (without immunoprecipitation).

Statistical analysis

All values are expressed as mean ± SEM. For animal behavior, a two-way ANOVA analyses with a Bonferroni post-hoc analysis was used. Unpaired t-test was used for the analysis of Western blot, pNPP, and immunohistochemistry data. A *p* value less than 0.05 was considered statistically significant. Statistical analyses were performed with GraphPad Prism 4 (GraphPad Software Inc., La Jolla, CA).

RESULTS

Effects of peripheral nerve injury and JWH015 treatment on spinal expression of MKP-1 and MKP-3

Four days after transection of the L5 spinal nerve, we observed a reduction of the withdrawal threshold for mechanical stimulation ipsilateral to the injury, which is indicative of allodynia (vs. baseline [before surgery] or sham group, Figure 1A). No change in withdrawal threshold was observed in the paw contralateral to the injury (data not shown), neither in ipsilateral and contralateral paws of rats receiving sham surgery four days after the injury (vs. base line or among groups, Figure 1A). The i.t. administration of vehicle neither changed the peripheral nerve injury-induced hypersensitivity 1 h after its administration nor modified the withdrawal thresholds in the contralateral paw on postoperative day 4 (Figure 1A). As we have previously shown,³⁰ the i.t. administration of JWH015 (50 μ g) was associated with higher withdrawal thresholds to mechanical stimulation 1 h after treatment when compared to vehicle treated rats, which is indicative of an antinociceptive effect (Figure 1A). This antinociceptive effect was not observed when JWH015 was administered i.t. in conjunction with triptolide (50 μ g), an MKP-1 and MKP-3 blocker,³¹ suggesting that spinal MKP-1 and MKP-3 may be part of the mechanism by which JWH015 induces antinociception (Figure 1A).

Four days after L5 nerve transection and in animals given vehicle, we observed a reduction of spinal MKP-1 (but not MKP-3) protein expression when compared to the sham-plus-vehicle group (Figures 1B–1D). The expression level of spinal MKP-1 and MKP-3 protein four days after L5 nerve transection in rats treated with JWH015 (same rats used for behavior) was higher than that observed in the L5 nerve transection group treated with vehicle (Figures 1B–1D). Expression of MKP-3 was higher in the L5 nerve transection and JWH015-treated group than in the sham-plus-vehicle group (Figures 1B and 1D). Spinal MKP-1 and MKP-3 protein levels were lower in L5 nerve transection and JWH015-plus-triptolide treated group compared to L5 nerve transection and JWH015-plus-vehicle group (Figures 1B–1D), confirming the blockade effect of triptolide on MKP-1 and MKP-3 expression.³¹

Spinal cord and cellular localization of MKP-1 and MKP-3

To determine the region of spinal cord dorsal horn where MKP-1 and MKP-3 expression were modulated by L5 nerve transection or JWH015, we performed immunohistochemistry studies in a separate set of animals. Expression of MKP-1 was observed throughout the whole dorsal horn in sham rats treated with vehicle (Figure 2A). We observed that MKP-1 expression in laminae I–II of dorsal horn spinal cord was reduced four days after L5 nerve transection compared to the sham group (both after 60 min of vehicle treatment, Figures 2A and 2B). The expression level of MKP-1 in laminae I–II of dorsal horn spinal cord was higher in L5 nerve transection and JWH015 treated group compared to L5 nerve transection and vehicle treated group (Figures 2A and 2B, 60 min after treatments). The expression of MKP-3 was observed mostly in deeper laminae of dorsal horn in sham rats treated with vehicle (Figure 2C). Though we did not observe changes in MKP-3 protein in the whole (dorsal and ventral horns) spinal cord ipsilateral to injury (Figures 1B and 1D) between sham and L5 nerve transection groups (both after 60 min of vehicle treatment) using Western blot analyses, we did observe a reduction of MKP-3 expression in laminae III–V of dorsal horn spinal cord of rats receiving L5 nerve transection when compared to rats receiving sham surgery (both after 60 min of vehicle treatment, Figures 2C and 2D). Expression of MKP-3 in laminae III–V of rats receiving L5 nerve transection surgery and JWH015 treatment was higher than in rats receiving L5 nerve transection surgery and vehicle treatment (Figures 2C and 2D, 60 min after treatment). These data suggest that our

quantitative approach using immunohistochemistry allows us to identify differences in MKP expression by performing analysis at different localized segments in spinal cord slices (laminae). When measured by Western blot analyses, the use of ventral and dorsal horn spinal tissue homogenates (hemisections) may dilute the localized segments of increased MKP expression to undetectable changes.

We also performed immunofluorescence studies and confocal microscopy to determine the cellular localization of spinal cord MKP-1 and MKP-3. Spinal cord neurons (NeuN expressing cells), astrocytes (GFAP expressing cells), and microglia (ED2 expressing cells) showed co-regionalization of MKP-1 expression in rats receiving sham surgery; this cellular expression pattern was not different in rats after L5 nerve transection surgery with either vehicle or JWH015 treatment (Figure 3, top panel). Spinal cord neurons (NeuN expressing cells) and microglia (ED2 expressing cells), but not astrocytes (GFAP expressing cells), showed co-regionalization of MKP-3 expression in rats receiving sham surgery; this cellular expression pattern was not different in rats receiving L5 nerve transection surgery with either vehicle or JWH015 treatment (Figure 3, bottom panel).

Effects of peripheral nerve injury and JWH015 treatment on phosphatase activity

General phosphatase activity was reduced in spinal cord (ipsilateral to injury) of rats receiving L5 nerve transection ($83.6 \pm 10.6\%$ of sham) when compared to that observed in spinal cord from rats receiving sham surgery ($100 \pm 4.4\%$)—both groups with vehicle treatment—and this was not changed following treatments with JWH015 plus vehicle ($76.3 \pm 4.4\%$ of sham) or JWH015 plus triptolide ($72.4 \pm 5.4\%$). To further determine the specific contribution of MKP-1 and MKP-3 in this general change in phosphatase activity, we performed selective immunoprecipitation experiments for MKP-1 or MKP-3 and measured their specific individual enzymatic activity.

Spinal cord (ipsilateral to injury) MKP-1 activity was reduced in rats receiving L5 nerve transection when compared to that observed in spinal cord from rats receiving sham surgery (both groups with vehicle treatment, Figure 4A), in accordance with the reduced MKP-1 protein level found in this group (Figures 1B and 1C, same rats used for behavior). MKP-1 activity was higher in the L5 nerve transection and JWH015-plus-vehicle group than in the L5 nerve transection and vehicle group (Figure 4A), in correlation with the higher levels of MKP-1 protein observed in this group (Figures 1B and 1C). Similarly, MKP-1 activity was higher in the L5 nerve transection and JWH015-plus-vehicle group than JWH015-plus-triptolide group (Figure 4A), in line with the MKP-1 expression blockade effects of triptolide of this group (Figures 1B and 1C).

Spinal cord (ipsilateral to injury) MKP-3 activity was similar in rats receiving L5 nerve transection or sham surgery (both groups with vehicle treatment, Figure 4B), in accordance with the lack of difference in MKP-3 protein level found in both groups (Figures 1B and 1D, same rats used for behavior). The activity of MKP-3 was higher in the L5 nerve transection and JWH015 plus vehicle group than in the L5 nerve transection and vehicle group (Figure 4B), in correlation with the higher levels of MKP-3 protein observed in this group (Figures 1B and 1D). However, the MKP-3 activity in the L5 nerve transection and JWH015 treated group was not different from the activity observed in the sham and vehicle treated group or in the L5 nerve transection and JWH015-plus-triptolide treated group (Figure 4B), out of step with the differential level of MKP-3 protein among these groups (Figures 1B and 1D). Together, these data suggest that changes in protein expression correlate with changes in enzymatic activity for spinal MKP-1, but changes in spinal MKP-3 protein expression do not necessarily translate to corresponding changes in enzymatic activity.

To further evaluate potential changes in MKP-1 and MKP-3 activity that may be independent of changes in protein expression, we quantified the amount of immunoprecipitated MKP-1 or MKP-3 protein and calculated their activity per microgram of MKP protein respectively. We observed no significant changes on a microgram-per-microgram basis among groups for both MKP-1 and MKP-3 activity, except for the L5 nerve transection groups treated with vehicle or JWH015, where MKP-1 and MKP-3 activity was higher in the JWH015 group vs. vehicle group (Figures 4C and 4D). These data further confirm that changes in MKP-1 expression correlate closely with changes in its enzymatic activity, and that changes in MKP-3 expression may be independent of changes in its enzymatic activity.

Functional association between JWH015 and downstream targets of MKP-1 and MKP-3

To further explore a functional association between JWH015 and MKPs, we studied the main targets of MKP-1 and MKP-3, namely the phosphorylated form of p38 (p-p38) and ERK-1/2 (pERK-1/2) respectively. As shown previously in rat neuropathic pain models, spinal cord expression (ipsilateral to injury) of p-p38 (Figures 5A and 5B) and p-ERK-1/2 (Figures 6A–6C) were enhanced following L5 nerve transection as compared to that observed in the sham group (both treated with vehicle). Spinal p-p38 and p-ERK-1/2 expression was reduced after L5 nerve transection with JWH015 treatment as compared to L5 nerve transection and vehicle or JWH015-plus-triptolide groups (Figures 5 and 6). These data further support the assumption that JWH015 induces its antinociceptive effects by inducing MKP-1 and MKP-3.

Role of cannabinoid type 2 receptors in modulation of MKP-1 and MKP-3 by JWH015

The antinociceptive effect of JWH015 (50 μ g, i.t.) in rats receiving L5 nerve transection was not observed when the cannabinoid type 2 receptor antagonist AM630 (50 μ g, i.t.) was administered concomitantly with JWH015 (Figure 7A). Similarly, the increased expression of spinal MKP-1 and MKP-3 observed in the L5 nerve transection and JWH015 group was not observed in the L5 nerve transection and JWH015-plus-AM630 group (Figure 7B–D). These data show that the effects of the CB2 receptor agonist JWH015 on spinal MKP-1 and MKP-3 actually depend upon its action on CB2 receptors.

DISCUSSION

The main findings of our study are, first, that peripheral nerve injury-induced allodynia and p38 and ERK phosphorylation are associated with a reduction in expression and/or activity of MKP-1 and MKP-3; second, that JWH015 induced an increase in the expression of spinal MKP-1 and MKP-3 in a rat model of neuropathic pain; third, that JWH015-induced spinal MKP-1 and MKP-3 increased expression resulted in a reduction of their main targets, p-p38 and p-ERK-1/2 in spinal cord; fourth, that JWH015-induced antinociception was blocked by a reduction of MKP-1 and MKP-3 expression and activity; and fifth, that JWH015 effects on spinal MKP-1 and MKP-3 expression depend on cannabinoid receptor type 2.

Association between the reduction of spinal MKPs and MAPK phosphorylation

The major regulators of MAPKs in peripheral inflammatory models are MKPs.²⁵ However, the potential role of MKPs in spinal cord following peripheral nerve injury has not been described. Our study shows that dysregulation of these major phosphatases in spinal cord following peripheral nerve injury may contribute to the pro-inflammatory/algescic milieu that underlies the spinal mechanisms of chronic allodynia. For example, it is well established that phosphorylation of the major MAPKs, p38 and ERK-1/2, is a pivotal spinal cord process that contributes to behavioral hypersensitivity in rodent models of neuropathic pain.¹⁵ However, the molecular mechanisms that allow dephosphorylation of these MAPKs or that limit their phosphorylation in spinal cord have not so far been described. Even though

phosphorylation of these MAPKs does not depend on MKPs but on kinases, the enzymatic potency of MKPs may be 100–1000-fold over kinases.¹⁴ Thus, modest changes in MKPs can produce profound effects in their substrates. Several studies indicate that MKPs rather than kinases determine the degree of MAPK phosphorylation.¹⁴ Therefore, the early reduction of spinal cord MKP-1 and MKP-3 expression and activity after peripheral nerve injury could facilitate the enhancement of spinal p-p38 and p-ERK-1/2 by a deficiency of their natural regulators, as has been shown in other systems.¹⁰

Association between JWH015-induced enhancement of spinal MKPs and reduction of the phosphorylated form of MAPKs

In line with the potential role of spinal MKPs in the regulation of MAPKs following peripheral nerve injury, we observed that restitution or augmentation of spinal MKP-1 and MKP-3 expression and activity induced by JWH015 was associated with a reduction of p-p38 and p-ERK-1/2, as we have previously demonstrated in primary rat microglial cultures.³¹ Additionally, we provide a functional link between JWH015's effects on MKPs and MAPKs expression by using triptolide (a pharmacological blocker of MKP-1 and MKP-3 expression). Triptolide reduced JWH015-induced MKP-1 and MKP-3 expression and enzymatic activity and, furthermore, inhibited reduction of spinal p-p38 and p-ERK-1/2 expression induced by JWH015. Our results strongly suggest that JWH015 reduces spinal p-p38 and p-ERK-1/2 by modulating MKP-1 and MKP-3 following peripheral nerve injury.

The main triggers of MKP expression are their own substrates, MAPKs.¹⁴ Our data suggest that this mechanism does not take place in spinal cord four days after peripheral nerve injury because a reduction in spinal MKP expression was observed when spinal MAPK expression was enhanced. Our results also show that CB2 receptor agonism restores or induces spinal MKP expression, likely by Histone 3 phosphorylation, as it has been previously shown.⁸

Our studies only include one time point after peripheral nerve injury, postoperative day 4, when behavioral hypersensitivity is established. However, our findings warrant a more thorough investigation of spinal MKPs following peripheral nerve injury. Our laboratory is currently performing studies to assess levels of spinal MKP expression at different time points after peripheral nerve injury (i.e., before and after postoperative day 4). These experiments will aid in clarifying whether spinal MKPs play a role only in the development phase (as observed in this study) or in both the development and maintenance phases of peripheral nerve injury-induced MAPK phosphorylation and allodynia.

Association between JWH015-induced enhancement of spinal MKPs and antinociception

Our studies have confirmed the antinociceptive effects of JWH015 in this rat model of neuropathic pain³⁰ and uncovered spinal cord molecular mechanisms of action of JWH015 involving MKP/MAPK pathways. The antinociceptive effects of spinal cannabinoid receptor type 2 agonism have been associated with a reduction of spinal cord p-p38 in other models of neuropathic pain,³⁶ but the mechanisms by which CB2 receptor agonists negatively regulate MAPK phosphorylation have not been described. We show that JWH015 reduces spinal p-p38 and p-ERK-1/2 in spinal cord in our model of neuropathic pain. Since spinal p-p38 and p-ERK-1/2 play a major role in the initiation and maintenance of mechanical allodynia following peripheral nerve injury,¹⁵ the negative regulation of these MAPKs by JWH015 is the simplest explanation for JWH015's antinociceptive effects in our studies. Our data indicate that the negative regulation of MAPK activation induced by JWH015 is due to the latter's effects on spinal MKPs, since triptolide blocked JWH015-induced antinociception (in parallel with triptolide blockade of MKP expression).

To our knowledge, this is the first time that an antinociceptive role of MKP-1 and MKP-3 has been described. In an independent study in our laboratory, we have observed that the single induction of spinal MKP-1 by in vivo transfection techniques is sufficient to induce antinociception in the L5 nerve transection rat model.²⁸ It is reasonable to suppose that spinal MKP-1 and MKP-3 are acting on their preferential targets (i.e., MKP-1 on p-p38, MKP-3 on pERK); however, our current studies cannot confirm this, and it is possible that single MKPs modulate several MAPKs. For example, it has been reported that MKP-1 induction in spinal cord is associated with a reduction in spinal-cord-injury-induced p-ERK and locomotor dysfunction.¹³ Additionally, our current studies do not rule out potential effects of JWH015 on MAPKs by MKP-independent mechanisms. Further studies with more specific approaches are warranted to elucidate the individual contribution of MKPs in neuropathic pain models and to evaluate cannabinoid modulation of MAPKs by MKP-independent mechanisms.

Cannabinoids, MKP/MAPK signaling, and pain

Clinical trials have shown that p-p38 plays a role in acute³⁵ and chronic⁴ pain in humans. Therefore, it is reasonable to conjecture that the natural regulators of p38, namely MKPs, may play a role in human pain. In fact, dexamethasone, which induces its anti-inflammatory effects by inducing MKP-1,^{1, 33, 39} improves the antinociceptive effects of other drugs in orthopedic⁵ and dental postsurgical pain in patients.²⁴ However, the clinical relevance of selective CB2 receptor agonists for the treatment of pain is not clear. The CB2 receptor agonist GW842166 has failed to reduce tooth extraction-induced postoperative pain in patients.⁴ Whether this lack of efficacy in patients is due to an insufficient modulation of MKPs or MAPKs (such as p-p38) is unknown. Other cannabinoid molecules, such as the endocannabinoid anandamide, have been shown to possess anti-inflammatory and neuroprotective effects in rodents by inducing MKP-1 and reducing MAPK activation.⁸ Whether drugs that enhance anandamide and induce antinociception in rodents^{6, 18, 32}—namely, inhibitors of fatty acid amide hydrolase, an anandamide-degradative enzyme—are effective in treating pain in humans remains to be shown. A prototype of this type of compound (PF-04457845) has been shown to enhance anandamide in humans while having a relatively safe side-effect profile.²⁶

CONCLUSIONS

Dysregulation of spinal MKPs may contribute to activation of MAPKs following peripheral nerve injury. Positive modulation of these phosphatases is sufficient to inactivate MAPKs and reduce mechanical allodynia. Our study uncovers the potential role of MKPs in pain mechanisms and supports further investigation of MKPs as potential targets for the treatment of pain.

Supplementary Material

Refer to Web version on PubMed Central for supplementary material.

References

1. Abraham SM, Lawrence T, Kleiman A, Warden P, Medghalchi M, Tuckermann J, Saklatvala J, Clark AR. Antiinflammatory effects of dexamethasone are partly dependent on induction of dual specificity phosphatase 1. *J Exp Med*. 2006; 203:1883–1889. [PubMed: 16880258]
2. Alkaitis, MS.; Ndong, C.; Landry, RP.; DeLeo, JA.; AR-SE. Reduced Antinociceptive Effect of Repeated Treatment with a Cannabinoid Receptor Type 2 Agonist in Cannabinoid-Tolerant Rats Following Spinal Nerve Transection. In: Racz, GB.; Noe, CE., editors. *Pain Management - Current Issues and Opinions*. InTech; 2012.

3. Alkaitis MS, Solorzano C, Landry RP, Piomelli D, DeLeo JA, Romero-Sandoval EA. Evidence for a role of endocannabinoids, astrocytes and p38 phosphorylation in the resolution of postoperative pain. *PLoS One*. 2010; 5:e10891. [PubMed: 20531936]
4. Anand P, Shenoy R, Palmer JE, Baines AJ, Lai RY, Robertson J, Bird N, Ostefeld T, Chizh BA. Clinical trial of the p38 MAP kinase inhibitor diltapimod in neuropathic pain following nerve injury. *Eur J Pain*. 2011; 15:1040–1048. [PubMed: 21576029]
5. Bani-Hashem N, Hassan-Nasab B, Pour EA, Maleh PA, Nabavi A, Jabbari A. Addition of intrathecal Dexamethasone to Bupivacaine for spinal anesthesia in orthopedic surgery. *Saudi J Anaesth*. 2011; 5:382–386. [PubMed: 22144925]
6. Chang L, Luo L, Palmer JA, Sutton S, Wilson SJ, Barbier AJ, Breitenbucher JG, Chaplan SR, Webb M. Inhibition of fatty acid amide hydrolase produces analgesia by multiple mechanisms. *Br J Pharmacol*. 2006; 148:102–113. [PubMed: 16501580]
7. Chaplan SR, Bach FW, Pogrel JW, Chung JM, Yaksh TL. Quantitative assessment of tactile allodynia in the rat paw. *J Neurosci Methods*. 1994; 53:55–63. [PubMed: 7990513]
8. Eljaschewitsch E, Witting A, Mawrin C, Lee T, Schmidt PM, Wolf S, Hoertnagl H, Raine CS, Schneider-Stock R, Nitsch R, Ullrich O. The endocannabinoid anandamide protects neurons during CNS inflammation by induction of MKP-1 in microglial cells. *Neuron*. 2006; 49:67–79. [PubMed: 16387640]
9. Gong Y, Xue B, Jiao J, Jing L, Wang X. Triptolide inhibits COX-2 expression and PGE2 release by suppressing the activity of NF-kappaB and JNK in LPS-treated microglia. *J Neurochem*. 2008; 107:779–788. [PubMed: 18761708]
10. Gozdz A, Vashishta A, Kalita K, Szatmari E, Zheng JJ, Tamiya S, Delamere NA, Hetman M. Cisplatin-mediated activation of extracellular signal-regulated kinases 1/2 (ERK1/2) by inhibition of ERK1/2 phosphatases. *J Neurochem*. 2008; 106:2056–2067. [PubMed: 18665890]
11. Hagg S, Alserius T, Noori P, Ruusalepp A, Ivert T, Tegner J, Bjorkegren J, Skogsberg J. Blood levels of dual-specificity phosphatase-1 independently predict risk for post-operative morbidities causing prolonged hospitalization after coronary artery bypass grafting. *Int J Mol Med*. 2011; 27:851–857. [PubMed: 21424112]
12. Hamm A, Krott N, Breibach I, Blindt R, Bosserhoff AK. Efficient transfection method for primary cells. *Tissue Eng*. 2002; 8:235–245. [PubMed: 12031113]
13. Huang H, Fan S, Ji X, Zhang Y, Bao F, Zhang G. Recombinant human erythropoietin protects against experimental spinal cord trauma injury by regulating expression of the proteins MKP-1 and p-ERK. *J Int Med Res*. 2009; 37:511–519. [PubMed: 19383246]
14. Jeffrey KL, Camps M, Rommel C, Mackay CR. Targeting dual-specificity phosphatases: manipulating MAP kinase signalling and immune responses. *Nat Rev Drug Discov*. 2007; 6:391–403. [PubMed: 17473844]
15. Ji RR, Gereau RWt, Malcangio M, Strichartz GR. MAP kinase and pain. *Brain Res Rev*. 2009; 60:135–148. [PubMed: 19150373]
16. Jin SX, Zhuang ZY, Woolf CJ, Ji RR. p38 mitogen-activated protein kinase is activated after a spinal nerve ligation in spinal cord microglia and dorsal root ganglion neurons and contributes to the generation of neuropathic pain. *J Neurosci*. 2003; 23:4017–4022. [PubMed: 12764087]
17. Jin Y, Hu D, Peterson EL, Eng C, Levin AM, Wells K, Beckman K, Kumar R, Seibold MA, Karungi G, Zoratti A, Gaggin J, Campbell J, Galanter J, Chapela R, Rodriguez-Santana JR, Watson HG, Meade K, Lenoir M, Rodriguez-Cintron W, Avila PC, Lanfear DE, Burchard EG, Williams LK. Dual-specificity phosphatase 1 as a pharmacogenetic modifier of inhaled steroid response among asthmatic patients. *J Allergy Clin Immunol*. 2010; 126:618–625. e611–612. [PubMed: 20673984]
18. Karbarz MJ, Luo L, Chang L, Tham CS, Palmer JA, Wilson SJ, Wennerholm ML, Brown SM, Scott BP, Apodaca RL, Keith JM, Wu J, Breitenbucher JG, Chaplan SR, Webb M. Biochemical and biological properties of 4-(3-phenyl-[1,2,4] thiazol-5-yl)-piperazine-1-carboxylic acid phenylamide, a mechanism-based inhibitor of fatty acid amide hydrolase. *Anesth Analg*. 2009; 108:316–329. [PubMed: 19095868]
19. Kawakami Y, Rodriguez-Leon J, Koth CM, Buscher D, Itoh T, Raya A, Ng JK, Esteban CR, Takahashi S, Henrique D, Schwarz MF, Asahara H, Izpisua Belmonte JC. MKP3 mediates the

- cellular response to FGF8 signalling in the vertebrate limb. *Nat Cell Biol.* 2003; 5:513–519. [PubMed: 12766772]
20. Kawasaki Y, Kohno T, Zhuang ZY, Brenner GJ, Wang H, Van Der Meer C, Befort K, Woolf CJ, Ji RR. Ionotropic and metabotropic receptors, protein kinase A, protein kinase C, and Src contribute to C-fiber-induced ERK activation and cAMP response element-binding protein phosphorylation in dorsal horn neurons, leading to central sensitization. *J Neurosci.* 2004; 24:8310–8321. [PubMed: 15385614]
 21. Kawasaki Y, Xu ZZ, Wang X, Park JY, Zhuang ZY, Tan PH, Gao YJ, Roy K, Corfas G, Lo EH, Ji RR. Distinct roles of matrix metalloproteases in the early- and late-phase development of neuropathic pain. *Nat Med.* 2008; 14:331–336. [PubMed: 18264108]
 22. Kim Y, Rice AE, Denu JM. Intramolecular dephosphorylation of ERK by MKP3. *Biochemistry.* 2003; 42:15197–15207. [PubMed: 14690430]
 23. Kizjakina K, Bryson JM, Grandinetti G, Reineke TM. Cationic glycopolymers for the delivery of pDNA to human dermal fibroblasts and rat mesenchymal stem cells. *Biomaterials.* 2012; 33:1851–1862. [PubMed: 22138032]
 24. Klongnoi B, Kaewpradub P, Boonsirisetth K, Wongsirichat N. Effect of single dose preoperative intramuscular dexamethasone injection on lower impacted third molar surgery. *Int J Oral Maxillofac Surg.* 2012; 41:376–379. [PubMed: 22209181]
 25. Korhonen R, Turpeinen T, Taimi V, Nieminen R, Goulas A, Moilanen E. Attenuation of the acute inflammatory response by dual specificity phosphatase 1 by inhibition of p38 MAP kinase. *Mol Immunol.* 2011; 48:2059–2068. [PubMed: 21764456]
 26. Li GL, Winter H, Arends R, Jay GW, Le V, Young T, Huggins JP. Assessment of the pharmacology and tolerability of PF-04457845, an irreversible inhibitor of fatty acid amide hydrolase-1, in healthy subjects. *Br J Clin Pharmacol.* 2012; 73:706–716. [PubMed: 22044402]
 27. Manetsch M, Che W, Seidel P, Chen Y, Ammit AJ. MKP-1: a negative feedback effector that represses MAPK-mediated pro-inflammatory signaling pathways and cytokine secretion in human airway smooth muscle cells. *Cell Signal.* 2012; 24:907–913. [PubMed: 22200679]
 28. Ndong C, Landry RP, Deleo JA, Romero-Sandoval EA. Mitogen activated protein kinase phosphatase-1 prevents the development of tactile sensitivity in a rodent model of neuropathic pain. *Mol Pain.* 2012; 8:34. [PubMed: 22540262]
 29. Oride A, Kanasaki H, Purwana IN, Miyazaki K. Possible involvement of mitogen-activated protein kinase phosphatase-1 (MKP-1) in thyrotropin-releasing hormone (TRH)-induced prolactin gene expression. *Biochem Biophys Res Commun.* 2009; 382:663–667. [PubMed: 19289102]
 30. Romero-Sandoval A, Nutile-McMenemy N, DeLeo JA. Spinal microglial and perivascular cell cannabinoid receptor type 2 activation reduces behavioral hypersensitivity without tolerance after peripheral nerve injury. *Anesthesiology.* 2008; 108:722–734. [PubMed: 18362605]
 31. Romero-Sandoval EA, Horvath R, Landry RP, DeLeo JA. Cannabinoid receptor type 2 activation induces a microglial anti-inflammatory phenotype and reduces migration via MKP induction and ERK dephosphorylation. *Mol Pain.* 2009; 5:25. [PubMed: 19476641]
 32. Russo R, Loverme J, La Rana G, Compton TR, Parrott J, Duranti A, Tontini A, Mor M, Tarzia G, Calignano A, Piomelli D. The fatty acid amide hydrolase inhibitor URB597 (cyclohexylcarbamic acid 3'-carbamoylbiphenyl-3-yl ester) reduces neuropathic pain after oral administration in mice. *J Pharmacol Exp Ther.* 2007; 322:236–242. [PubMed: 17412883]
 33. Shipp LE, Lee JV, Yu CY, Pufall M, Zhang P, Scott DK, Wang JC. Transcriptional regulation of human dual specificity protein phosphatase 1 (DUSP1) gene by glucocorticoids. *PLoS One.* 2010; 5:e13754. [PubMed: 21060794]
 34. Srivastava N, Sudan R, Saha B. CD40-modulated dual-specificity phosphatases MAPK phosphatase (MKP)-1 and MKP-3 reciprocally regulate Leishmania major infection. *J Immunol.* 2011; 186:5863–5872. [PubMed: 21471446]
 35. Tong SE, Daniels SE, Black P, Chang S, Protter A, Desjardins PJ. Novel p38alpha Mitogen-Activated Protein Kinase Inhibitor Shows Analgesic Efficacy in Acute Postsurgical Dental Pain. *J Clin Pharmacol.* 2012; 52:717–728. [PubMed: 21659629]

36. Toth CC, Jedrzejewski NM, Ellis CL, Frey WH 2nd. Cannabinoid-mediated modulation of neuropathic pain and microglial accumulation in a model of murine type I diabetic peripheral neuropathic pain. *Mol Pain*. 2010; 6:16. [PubMed: 20236533]
37. Wen YR, Suter MR, Ji RR, Yeh GC, Wu YS, Wang KC, Kohno T, Sun WZ, Wang CC. Activation of p38 mitogen-activated protein kinase in spinal microglia contributes to incision-induced mechanical allodynia. *Anesthesiology*. 2009; 110:155–165. [PubMed: 19104183]
38. Zhao Q, Shepherd EG, Manson ME, Nelin LD, Sorokin A, Liu Y. The role of mitogen-activated protein kinase phosphatase-1 in the response of alveolar macrophages to lipopolysaccharide: attenuation of proinflammatory cytokine biosynthesis via feedback control of p38. *J Biol Chem*. 2005; 280:8101–8108. [PubMed: 15590669]
39. Zhou Y, Ling EA, Dheen ST. Dexamethasone suppresses monocyte chemoattractant protein-1 production via mitogen activated protein kinase phosphatase-1 dependent inhibition of Jun N-terminal kinase and p38 mitogen-activated protein kinase in activated rat microglia. *J Neurochem*. 2007; 102:667–678. [PubMed: 17403137]

PERSPECTIVE

Mitogen-activated protein kinases (MAPKs) are pivotal in the development of chronic allodynia in rodent models of neuropathic pain. A cannabinoid type 2 receptor agonist, JWH015, reduced neuropathic allodynia in rats by reducing MAPK phosphorylation and inducing spinal MAPK phosphatases 1 and 3, the major regulators of MAPKs.

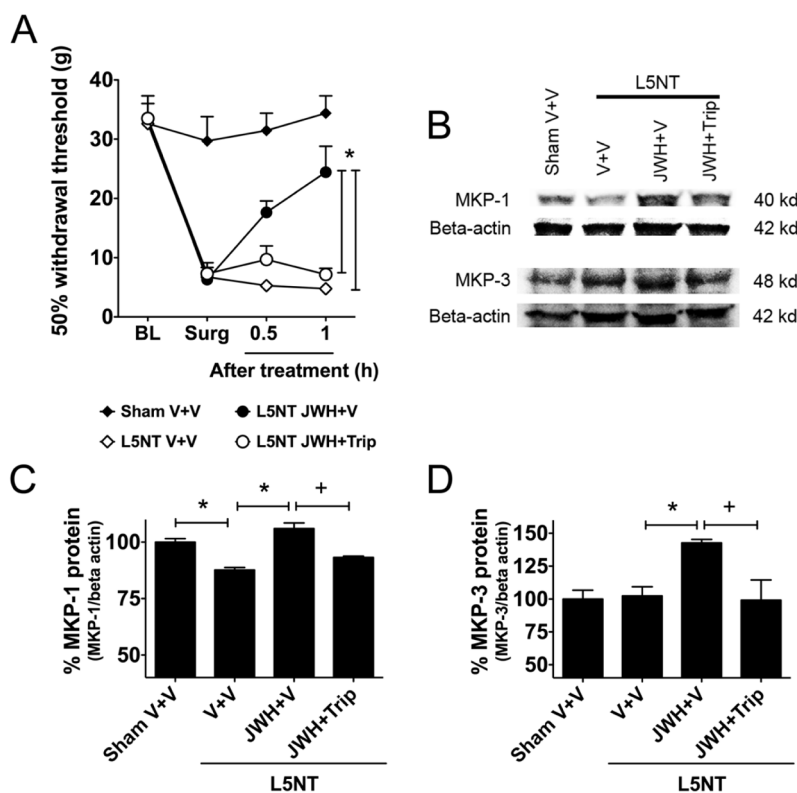


Figure 1. Effects of L5 nerve transection and JWH015 on behavioral hypersensitivity and MKP-1 and MKP-3 protein expression

(A) 50% paw withdrawal threshold assessed at baseline (BL), four days after surgery (Surg), and 0.5 h and 1 h after treatment in rats undergoing L5 nerve transection surgery (L5NT) and treated i.t. with vehicle (V, $n = 3$), JWH015 (JWH, 50 μg) plus vehicle ($n = 6$), and JWH015 (50 μg) plus triptolide (Trip, $n = 6$), and in rats undergoing sham surgery and treated with i.t. vehicle ($n = 3$). Two-way ANOVA + Bonferroni post hoc analysis, $*p < 0.05$ Sham V+V or L5NT JWH+V compared to L5NT V+V; $+p < 0.05$ L5NT JWH+Trip compared to L5NT JWH+V. (B) Representative Western blot images of L5 spinal cord for MKP-1, MKP-3, or Beta-actin 1 h after i.t. treatments. (C) Quantification of western blot images presented as % of MKP-1 protein expression of sham V+V group ($n = 3$ per group). Unpaired t-test, $*p < 0.05$ L5NT JWH+V compared to L5NT V+V or Sham V+V; $+p < 0.05$ L5NT JWH+Trip compared to L5NT JWH+V. (D) Quantification of western blot images presented as % of MKP-3 protein expression of sham V+V group ($n = 3$ per group). Unpaired t-test, $*p < 0.05$ L5NT JWH+V compared to Sham V+V or L5NT V+V; $+p < 0.05$ L5NT JWH+Trip compared to L5NT JWH+V. Results are reported as mean \pm SEM.

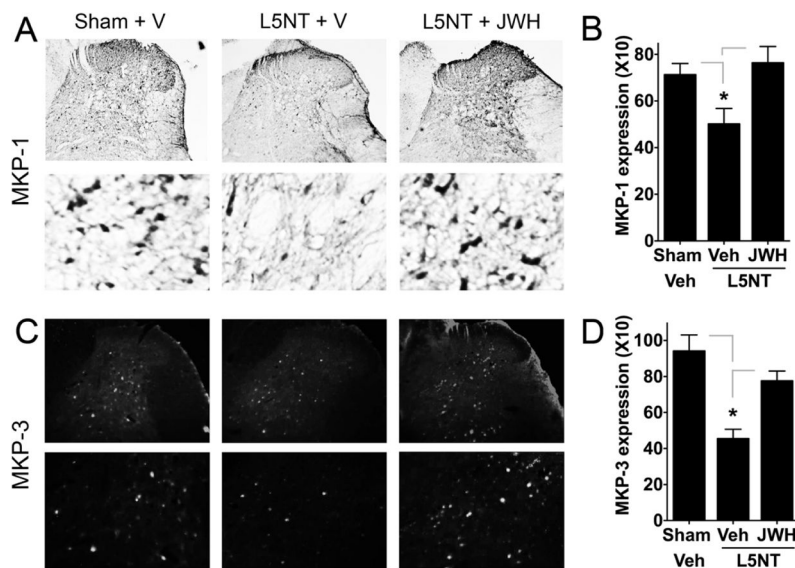


Figure 2. Quantification and localization of MKP-1 or MKP-3 protein expression in spinal cord dorsal horn

(A) Representative images displaying MKP-1 staining in dorsal horn of L5 spinal cord from rats undergoing L5 nerve transection (L5NT) and treated with vehicle (V) or JWH015 (JWH) and in rats undergoing sham surgery and treated with vehicle. Bottom panel are laminae I–II images magnified from dorsal horn of respective images in top panel. (B) Quantification of MKP-1 staining in laminae I–II of dorsal horn of L5 spinal cord from rats undergoing L5 nerve transection (L5NT) and treated with vehicle (Veh, $n = 4$) or JWH015 (JWH, $n = 4$) and in rats undergoing sham surgery and treated with vehicle ($n = 4$). Unpaired t-test, $*p < 0.05$ L5NT+Veh compared to L5NT+JWH or Sham+Veh. (C) Representative images displaying MKP-3 staining in dorsal horn of L5 spinal cord from rats undergoing L5 nerve transection (L5NT) and treated with vehicle (V) or JWH015 (JWH) and in rats undergoing sham surgery and treated with vehicle. Bottom panel shows laminae III–V images magnified from dorsal horn of respective images in top panel. (D) Quantification of MKP-3 staining in laminae III–V of dorsal horn of L5 spinal cord from rats undergoing L5 nerve transection (L5NT) and treated with vehicle (Veh, $n = 4$) or JWH015 (JWH, $n = 4$) and in rats undergoing sham surgery and treated with vehicle ($n = 3$). Unpaired t-test, $*p < 0.05$ L5NT+Veh compared to L5NT+JWH or Sham+Veh. Results are reported as mean \pm SEM.

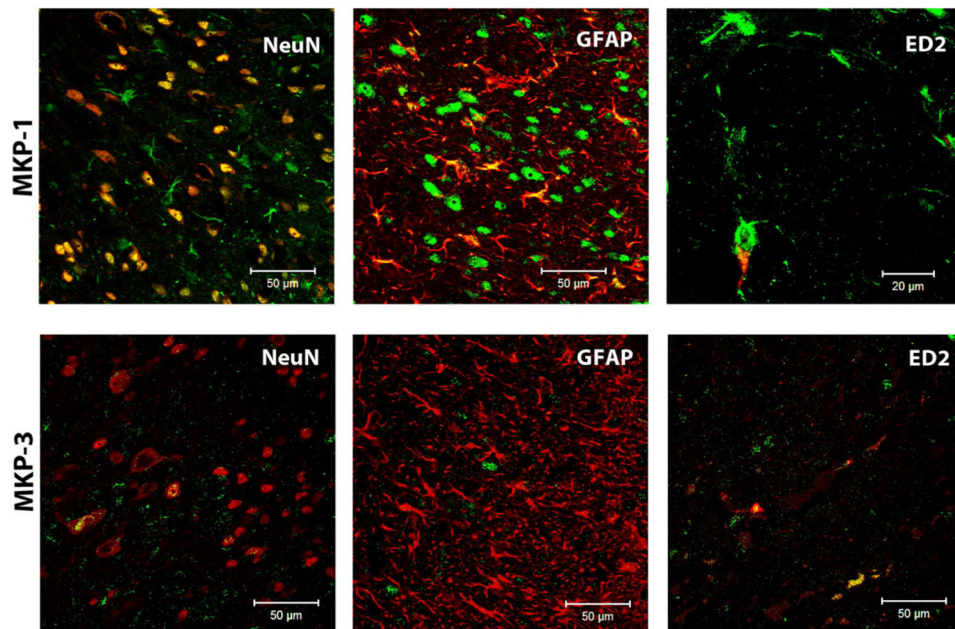


Figure 3. Confocal images of MKP-1 and MKP-3 and markers for neurons, astrocytes, and microglia

Top Panel: MKP-1 staining (green) in NeuN-expressing neurons (red), GFAP-expressing astrocytes (red), or ED2-expressing microglia (red) in the L5 spinal cord of rats undergoing L5 nerve transection and treated with JWH015. Bottom Panel: MKP-3 staining (green) in NeuN-expressing neurons (red), GFAP-expressing astrocytes (red), or ED2-expressing microglia (red) in the L5 spinal cord of rats undergoing L5 nerve transection and treated with JWH015.

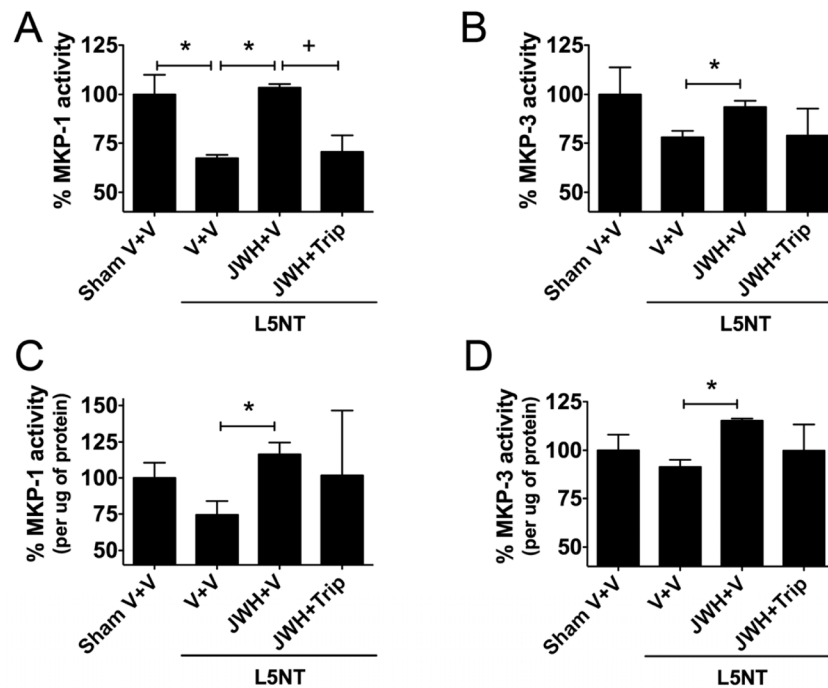


Figure 4. Effects of L5 nerve transection and JWH015 on MKP-1 or MKP-3 enzymatic activity (A) Total % MKP-1 enzymatic activity in L5 spinal cord of rats undergoing L5 nerve transection surgery (L5NT) and treated i.t. with vehicle (V, $n = 3$), JWH015 (JWH, 50 μg) plus vehicle ($n = 3$), or JWH015 (50 μg) plus triptolide (Trip, 50 μg , $n = 3$) and in rats undergoing sham surgery and treated with i.t. vehicle ($n = 3$). Unpaired t-test, $*p < 0.05$ Sham V+V or L5NT JWH+V compared to L5NT V+V; $+p < 0.05$ L5NT JWH+Trip compared to L5NT JWH+V. (B) Total % MKP-3 enzymatic activity in L5 spinal cord of rats undergoing L5 nerve transection surgery and treated i.t. with vehicle ($n = 3$), JWH015 (50 μg) plus vehicle ($n = 3$), or JWH015 (50 μg) plus triptolide (50 μg , $n = 3$) and in rats undergoing sham surgery and treated with i.t. vehicle ($n = 3$). Unpaired t-test, $*p < 0.05$ L5NT JWH+V compared to L5NT V+V. (C) % of enzymatic activity per microgram of MKP-1 protein in L5 spinal cord of rats undergoing L5 nerve transection surgery and treated i.t. with vehicle ($n = 5$), JWH015 (50 μg) plus vehicle ($n = 3$), or JWH015 (50 μg) plus triptolide (50 μg , $n = 3$) and in rats undergoing sham surgery and treated with i.t. vehicle ($n = 5$). Unpaired t-test, $*p < 0.05$ L5NT JWH+V compared to L5NT V+V. (D) % of enzymatic activity per microgram of MKP-3 protein in L5 spinal cord of rats undergoing L5 nerve transection surgery and treated i.t. with vehicle ($n = 3$), JWH015 (50 μg) plus vehicle ($n = 3$), or JWH015 (50 μg) plus triptolide (50 μg , $n = 3$) and in rats undergoing sham surgery and treated with i.t. vehicle ($n = 3$). Unpaired t-test, $*p < 0.05$ L5NT JWH+V compared to L5NT V+V. Results are reported as mean \pm SEM.

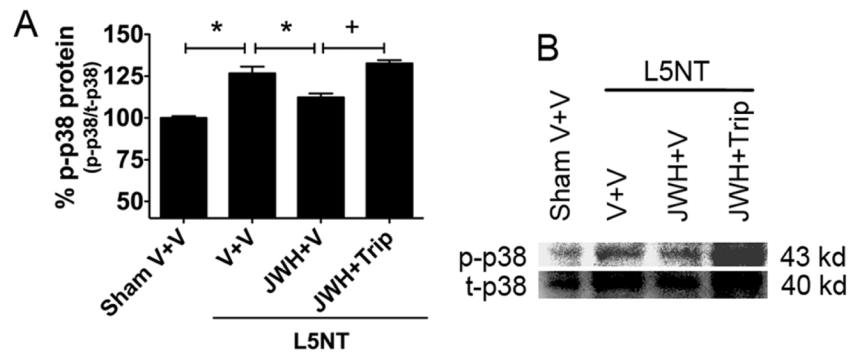


Figure 5. Effects of JWH015 on L5 nerve transection-induced p-p38 expression

(A) Quantification of p-p38 expression in L5 spinal cord of rats undergoing sham or L5 nerve transection and treated with vehicle, JWH015, and/or triptolide ($n = 3$ per group). Unpaired t-test, $*p < 0.05$ Sham V+V or L5NT JWH+V compared to L5NT V+V; $+p < 0.05$ L5NT JWH+Trip compared to L5NT JWH+V. (B) Representative Western blot image for p-p38 and total p38 (t-p38) expression in L5 spinal cord of rats undergoing sham or L5 nerve transection and treated with vehicle, JWH015, and/or triptolide. Results are reported as mean \pm SEM.

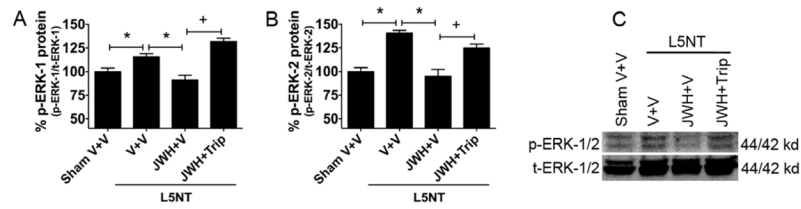


Figure 6. Effects of JWH015 on L5 nerve-transection-induced p-ERK-1/2 expression

Quantification of p-ERK-1 (A) and pERK-2 (B) expression in L5 spinal cord of rats undergoing sham or L5 nerve transection and treated with vehicle, JWH015, and/or triptolide ($n = 3$ per group). Unpaired t-test, $*p < 0.05$ Sham V+V or L5NT JWH+V compared to L5NT V+V; $+p < 0.05$ L5NT JWH+Trip compared to L5NT JWH+V. (C) Representative Western blot image for p-ERK-1/2 and total ERK-1/2 (t-ERK-1/2) expression in L5 spinal cord of rats undergoing sham or L5 nerve transection and treated with vehicle, JWH015, and/or triptolide. Results are reported as mean \pm SEM.

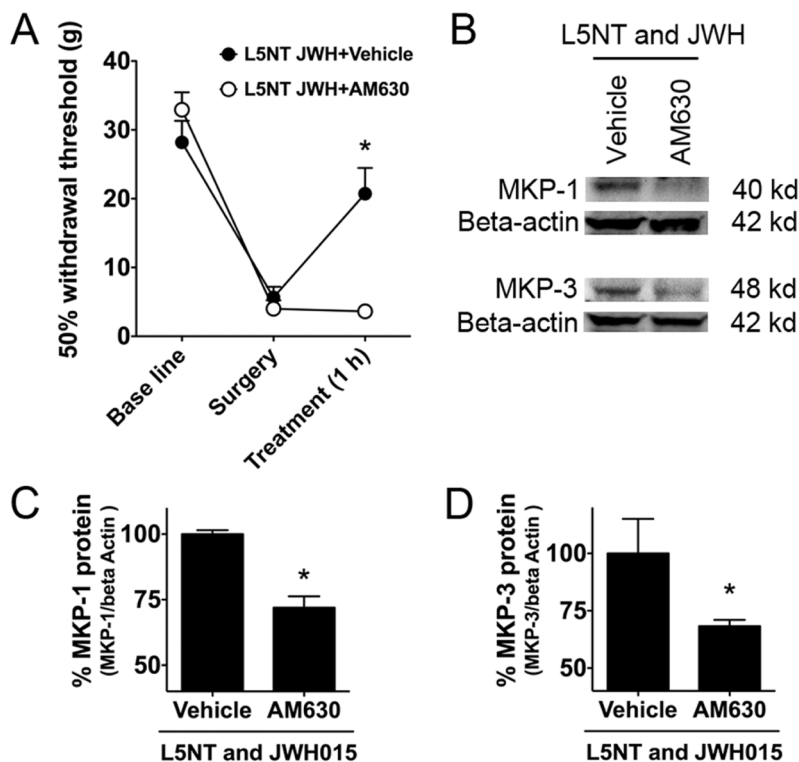


Figure 7. Effects of AM630 on JWH015-induced antinociception and MKP-1 and MKP-3 expression

(A) 50% paw withdrawal threshold assessed at baseline (BL), 4 days after surgery, and 1 h after treatment in rats undergoing L5 nerve transection surgery (L5NT) and treated i.t. with JWH015 (JWH, 50 μ g) plus vehicle ($n = 6$) or JWH015 (50 μ g) plus AM630 (50 μ g, $n = 4$). Two-way ANOVA + Bonferroni post hoc analysis, $*p < 0.05$ L5NT JWH+AM630 compared to L5NT JWH+Vehicle. (B) Representative Western blot images of MKP-1, MKP-3, or Beta-actin in L5 spinal cord from rats undergoing L5 nerve transection and treated with JWH015 and vehicle or AM630. (C) Quantification of MKP-1 expression in L5 spinal cord from rats undergoing L5 nerve transection and treated with JWH015 and vehicle or with JWH015 and AM630 ($n = 4$ per group). (D) Quantification of MKP-3 expression in L5 spinal cord from rats undergoing L5 nerve transection and treated with JWH015 and vehicle or with JWH015 and AM630 ($n = 4$ per group). Unpaired t-test, $*p < 0.05$ L5NT JWH+AM630 compared to L5NT JWH+Vehicle in C, and D. Results are reported as mean \pm SEM.